Two-dimensional Characterization of Window Contamination in Selective Laser Sintering

Doug Sassaman[1], Peter Hall[2], Scott Fish[1], Joseph Beaman[1]

[1]Department of Mechanical Engineering
Cockrell School of Engineering, the university of Texas at Austin, Austin, TX 78705
[2]Stratasys Direct Manufacturing, Belton, TX 76513

Abstract

Most Laser Sintering machines suffer from an issue where it is hypothesized that hot gases produced during the laser sintering process collect on the Zinc selenide (ZnSe) window separating the build chamber from the environment. This contamination has previously been shown to reduce delivered laser power by up to 10%, and necessitate frequent cleaning and replacement of the windows. A power meter was constructed in order to perform ex-situ measurements of laser attenuation at various locations on the window. Identical builds were performed using fire-retardant nylon 11 on a DTM Sinterstation 2500, and the windows were measured before and after each build. Results indicate that contamination is not uniform on the window, and may cause a variation in laser attenuation up to 3.5%±0.25% depending on scanning location. It is also shown here that the contamination patterns are not repeatable from build to build, even if performed on the same machine.

Background

The laser sintering (LS) process is extremely sensitive to the amount of energy delivered to the build surface; subtle variations in pre-sintering temperature across the powder bed can result in reduced post-sintering part strength and quality [1]. Recent research has been conducted on reducing the thermal gradient of the pre-sintered powder bed surface by means of closed-loop control of the radiative heating elements [2]. To further reduce the variation of delivered energy, a method for controlling the laser power based on pre-sintering temperatures was developed and proven successful [3]. In summary, much research has been performed on reducing, and correcting for, thermal gradients across and into the powder surface. However, even assuming a perfectly uniform pre-sintering powder bed temperature, one unassailable issue still remains: the contamination of the laser window and its effects on delivered laser power.

In most LS machines, the build chamber is separated from the optical cavity by means of a high transparency "window", shown in Figure 1. In the case of machines employing a CO_2 laser, this window is often made of ZnSe. Contamination of this laser window is a ubiquitous issue in industry, and necessitates frequent cleaning and replacement of the expensive windows.

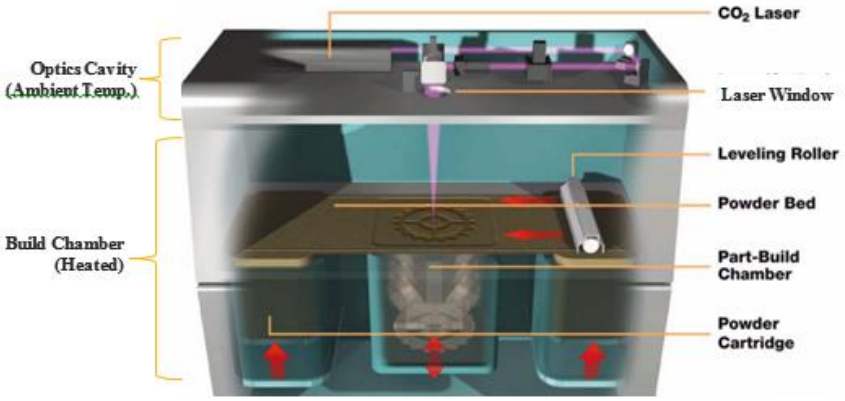

Figure 1: Schematic of 3D Systems Sinterstation SLS Machine [4]

The standing hypothesis for this contamination is that the high temperatures of LS produce an outgassing of the polymer, which circulates through the build chamber and eventually condenses on the laser window. One particular explanation for this is that during the LS of polymer, particularly polyamide (PA) 11 & 12, water vapor is produced from the post-condensation reaction between two PA monomers [5], Figure 2. This water vapor may act as the contamination "transporter", however, the exact mechanisms for this contamination are still largely unknown.

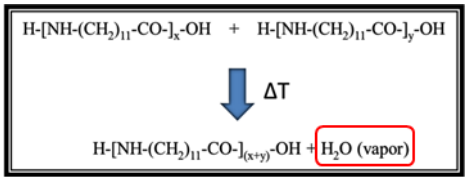

Figure 2: Post-condensation reaction between two polyamide monomers [5]

A headspace Gas Chromatography/Mass Spectrometry (HS/GC/MS) analysis of ALM D80 and FR-106 Nylon 11 powders was performed for Harvest Technologies (now Stratasys Direct Manufacturing, Belton, TX). This analysis showed that lactam 11, a residual monomer of nylon 11, was released at 140°C, 220°C, 300°C; note that the melt temperature of these materials is around 186-189°C [6, 7]. It is unclear if lactam 11 is a component of laser window contamination, however if it is, the above results would confer with the temperature theory and may indicate that contamination occurs even during the machine pre-heating process and not only during LS.

To minimize thermal gradients across the build surface, temperature in the build chamber is elevated by a series of conductive and radiative heaters (quartz lamps), a method that has been in use since the early days of SLS. The optical cavity, however, remains near ambient temperature, also indicated in Figure 1. The result is a thermal gradient across the thickness of the laser window, likely resulting in a laser window surface temperature lower than the build chamber "air" temperature. Fulcher et al. suspected that this cooler window surface was a main driver for "condensation" of the hot gasses which they speculated to be the root cause of contamination. A heated laser window was designed by Fulcher et al. and shown to reduce laser power attenuation due to contamination significantly; thereby confirming that window temperature plays a large roll in this contamination [8]. Figure 3 shows that with a standard, non-

heated window, after three builds laser power was attenuated 20-25%, while with the heated window, after three builds the laser power was attenuated 3-5% [8].

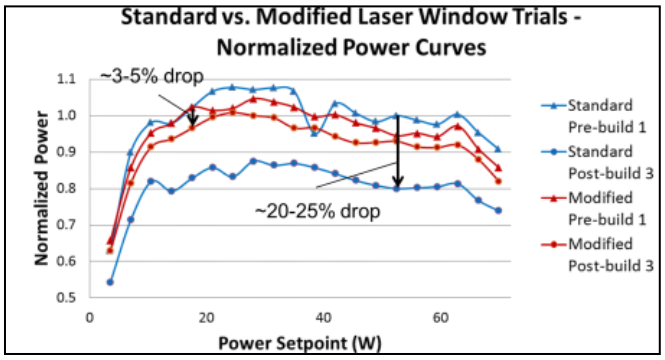

Figure 3: Laser power attenuation for standard and modified laser window [8]

In many machines, the build chamber is purged with heated nitrogen, often onto or very near the laser window, to aid in convection and dehumidifying the chamber. Some evidence has been presented that, although typically heated to 90-100°C, the actual temperature of nitrogen reaching the build chamber is closer to 50°C and may actually be causing some window contamination [5]. Other work has shown that purge gas applied through ports near the laser window may reduce part bed temperature gradient by removing the stagnation region above the build surface. Diller et al. also claimed that the convection pattern forms early in the warm-up cycle and remains fairly constant during a build [9], Figure 4. If the previous claim holds true that a residual monomer is released during the pre-heat stage of a build, the convection pattern shown in Diller et al. may explain any contamination occurring before LS actually begins. The present work aims to present results in support of chamber flows aiding in the contamination of laser windows.

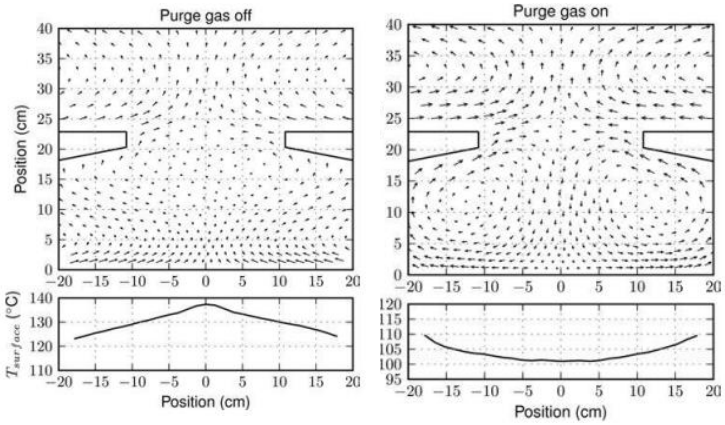

Figure 4: Steady-state convection, warm-up after 1600sec, vectors of gas velocity at mesh nodes. Lower axes show powder bed surface temperature, initial temp 60C [9]

During the design of the aforementioned heated window, Fulcher et al. found that "residue buildup appears to cause a percentage drop in laser power, rather than a constant drop". To clarify; during build #1, contamination caused a ~10% attenuation of laser power before/after, while the shorter build #3 caused only ~2-3% attenuation of laser power before/after, Figure 5 [5]. As will be presented later in this work, contamination may be correlated with the number of

layers in a build rather than build volume or time; thus confirming the earlier speculations of Fulcher et al.

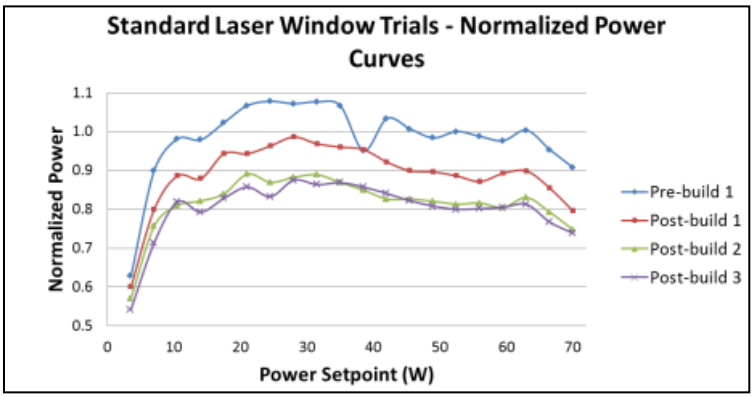

Figure 5: Measured laser power before and after 3 builds in Sinterstation 2500 at SDM; builds 1 & 2: 16" high, build 3: 6" high [5]

In an attempt to quantify laser window contamination during each build, the authors of this report discovered [qualitatively] that contamination was not uniform across the window (2D) and did not seem to be repeatable from build-to-build or machine-to-machine. This is problematic because current industrial practice is to take one single point-measurement near the center of the window using a commercial power meter to determine if the window needs to be cleaned or replaced. To further investigate, this work presents a 2D, ex-situ, measurement strategy to improve upon the industry standard, and provides evidence in support of window contamination being non-repeatable and non-uniform. This work also aims to tie together the temperature-based theory of window contamination with one also considering chamber/powder spreading effects, and ultimately purports that contamination is more closely related to number of layers than to other build parameters.

Experimental Design

All builds described in this report were performed at Stratasys Direct Manufacturing (SDM) (Belton, TX) with a 3D Systems Sinterstation 2500. Unless otherwise noted, the material used was ALM FR-106, a fire-retardant nylon 11 common in additive manufacture. Laser power was measured before and after each build using an Ophir Orion/TH/FLA-250A power meter. To do so, the power meter was placed near the center of the build area, the machine's laser fired manually at a nominal value, and the power recorded approximately 3 seconds after the "highest" power was observed on the power meter head unit. This is also the current method SDM uses to determine if a window needs to be cleaned or replaced during normal production. The laser windows were cleaned after each build, unless otherwise noted, using a proprietary mixture of acids before beginning subsequent builds.

As previously mentioned, the single-point power measurements described above were speculated to be insufficient, so a 2D measurement strategy is presented here. A low-cost power meter was constructed using a visible-light red laser and a photodiode, Figure 6, to allow for offline measurements of laser windows. The laser power was modulated at 100Hz using an Arduino Mega 2560, and the signal was filtered to remove DC noise such as ambient fluorescent

lighting. The photodiode current was converted to voltage and measured in LabVIEW. Both components were secured in a fixture ensuring perpendicularity between the laser beam and photodiode surface.

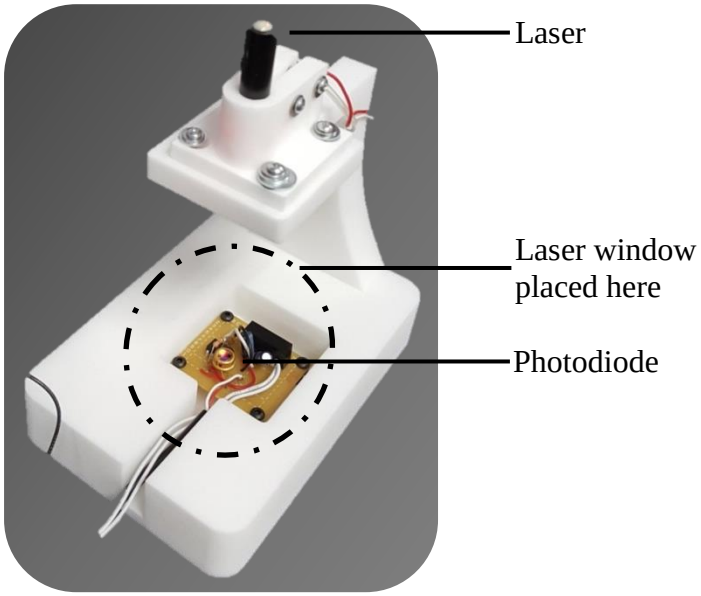

Figure 6: Low cost laser/photodiode power meter

Before and after each round of laser window measurements, the above device was powered on for 10 minutes with no window between the laser and photodiode (ambient light present) and the voltages recorded. These "drift" measurements were used to establish device uncertainty by (1), where X_i is the "true" voltage from the photodiode, X_m is the measured voltage from the photodiode, t is the Student's t-statistic, S_N is the standard deviation of the set of N observations [10].

$$X_i = X_m \mp t * \frac{S_N}{\sqrt{N}} \quad (1)$$

To measure laser window contamination using the above apparatus, each laser window was removed from the machine and placed on the fixture as indicated. A measurement grid was established (Figure 7), and the window was moved manually to take a measurement at each point. The laser was fired for ten seconds at each measurement point, thus resulting in roughly 10 data points at each location. Note that the transmission values of the ZnSe laser window are nearly identical for the visible red laser (632nm) used in offline testing and the CO_2 laser (10.6μm) used during LS. Also note that the grid paper was removed prior to acquiring data.

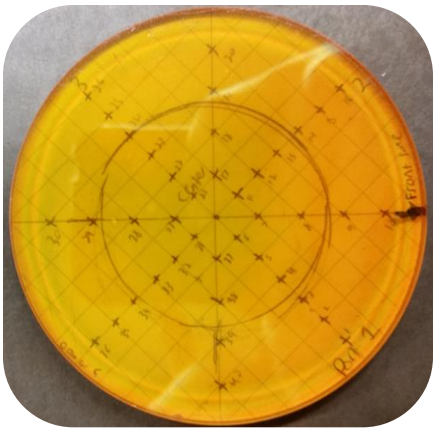

Figure 7: Zinc selenide laser window overlaid on measurement grid

Results

Eight normal production builds were performed at SDM and their parameters given in Table 1. Laser power was measured before and after each build with an Ophir power meter as described previously. Builds 1-5 were all unique, while builds 6-8 were identical. For builds 6-8, a brand new window was inserted into the machine before each build, and the same part was built on the same machine each time. The results are also presented in graphical form in Figure 8.

Table 1: SLS Build parameters and measured laser powers

Build #	Machine	Material	Date (Start)	Build Time (hrs)	Build Height (in)	Laser Setpoint	Laser Power (Before)	Laser Power (After)	% Degradation
1	F78	Fire Retardant Nylon 11	2/10/2017	43.50	12.82	46	46.3	44.1	4.75
2	G49	Fire Retardant Nylon 11	2/12/2017	40.23	16.91	41	38.6	35.6	7.77
3	F78	Fire Retardant Nylon 11	2/13/2017	38.54	14.25	46	46.6	43.9	5.79
4	F78	Fire Retardant Nylon 11	2/15/2017	39.36	14.25	46	46.9	44.4	5.33
5	G49	Fire Retardant Nylon 11	2/14/2017	39.41	16.26	41	38.9	36.3	6.68
6	Same	ALM FR-106	10/13/2017	39.30	14.20	41	39.6	38.0	4.04
7		ALM FR-106	10/13/2017	39.30	14.20	41	41.0	40.3	1.71
8		ALM FR-106	10/13/2017	39.30	14.20	41	39.8	39.5	0.75

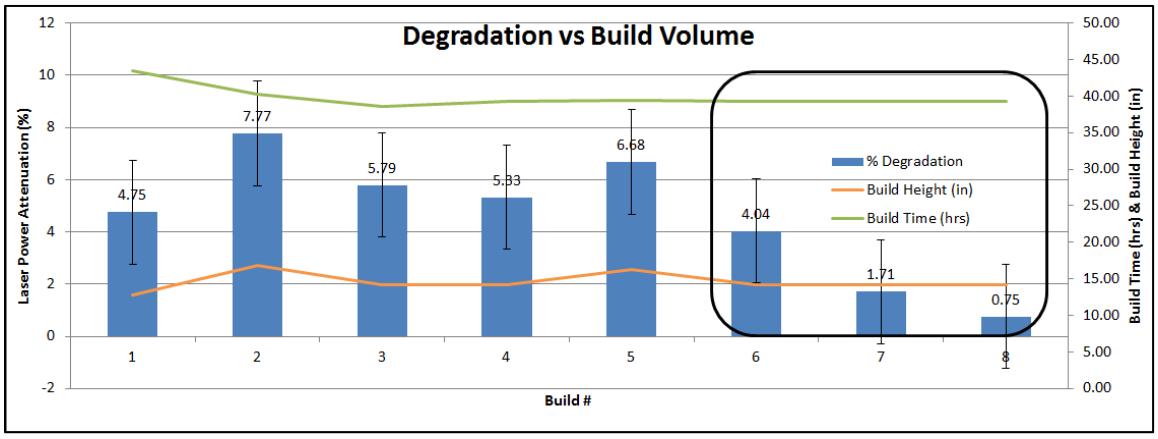

Figure 8: Correlation between laser power attenuation and build parameters

Builds 1-5 were performed initially and showed some correlation between contamination and build height, thus lending some evidence to this hypothesis. However, builds 6-8 show no

correlation with any build parameters, but are analyzed further below. The black error bars in Figure 8 represent the manufacturers stated uncertainty of the power meter used to measure. In order to improve upon this ±3%, more than 10 measurements would need to be taken at the center of each window [10].

The low-cost power meter described in the Experimental Design section was used to further analyze builds 7 and 8 by measuring at each point shown in Figure 7. Contour plots, shown in Figure 9, were created by interpolating between each measurement point and normalizing. These plots show attenuation relative to a clean window; i.e., a value of 1.0 corresponds to 100% transmissive to the visible red laser (632nm) and a value less than 1.0 represents a point that is contaminated. The left column shows windows from build 7 & 8, both brand new, measured before the build. The right column shows the same windows after undergoing identical builds on the same machine. The white region encircled by the light blue line represents the region where the window is clamped in its housing and is irrelevant here.

As mentioned, a robust device uncertainty analysis was performed for the low-cost power meter, such that when following the measurement technique outlined above, each stated value is ±0.51% (95% confidence interval) [10]. When applying this uncertainty to Figure 9, one can deduce, for example, that a value of 0.92 would have an uncertainty of roughly ±0.005.

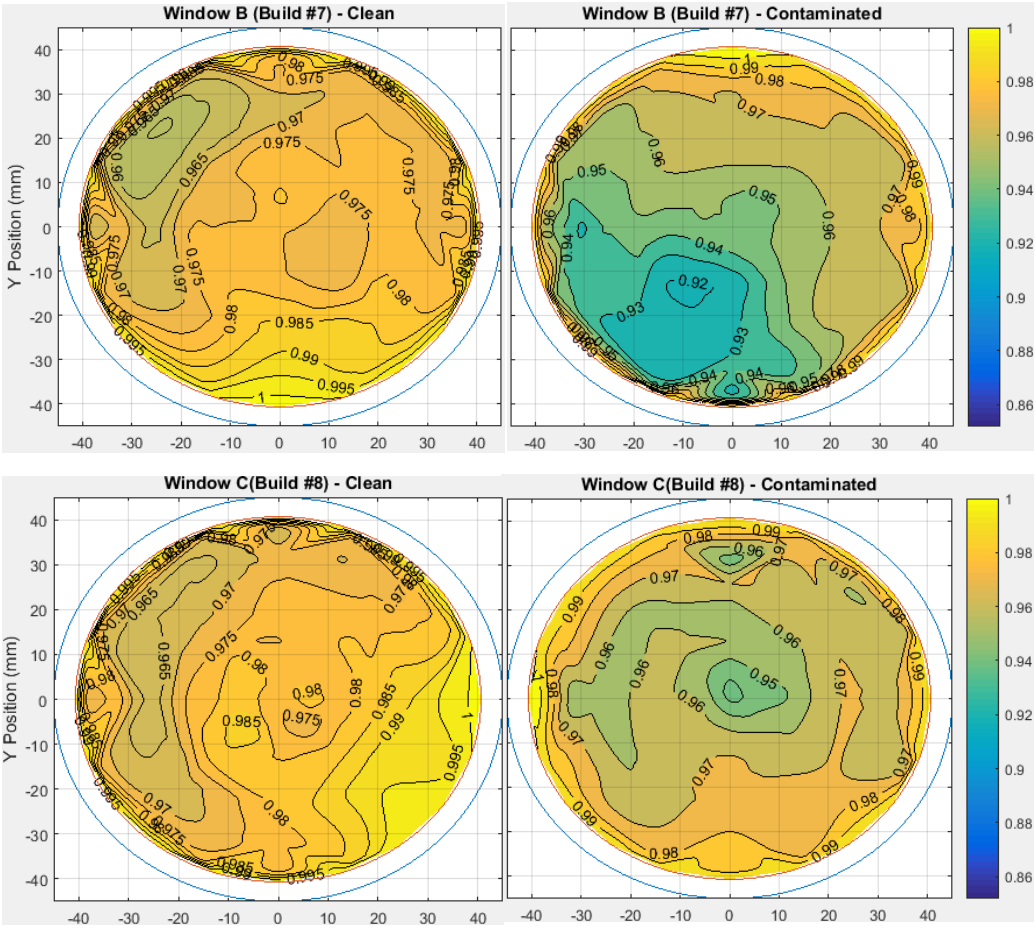

Figure 9: Contour plots of laser power attenuation due to contamination for builds 7 & 8

It is apparent from Figure 9 that laser window contamination is not uniform in 2D and that the contamination pattern is different between the two plots; thus indicating that contamination is likely not repeatable form build-to-build or machine-to-machine. In order to better visualize any trends, additional contour plots were created that show the % change in attenuation before and after each build for both windows; see Figure 10.

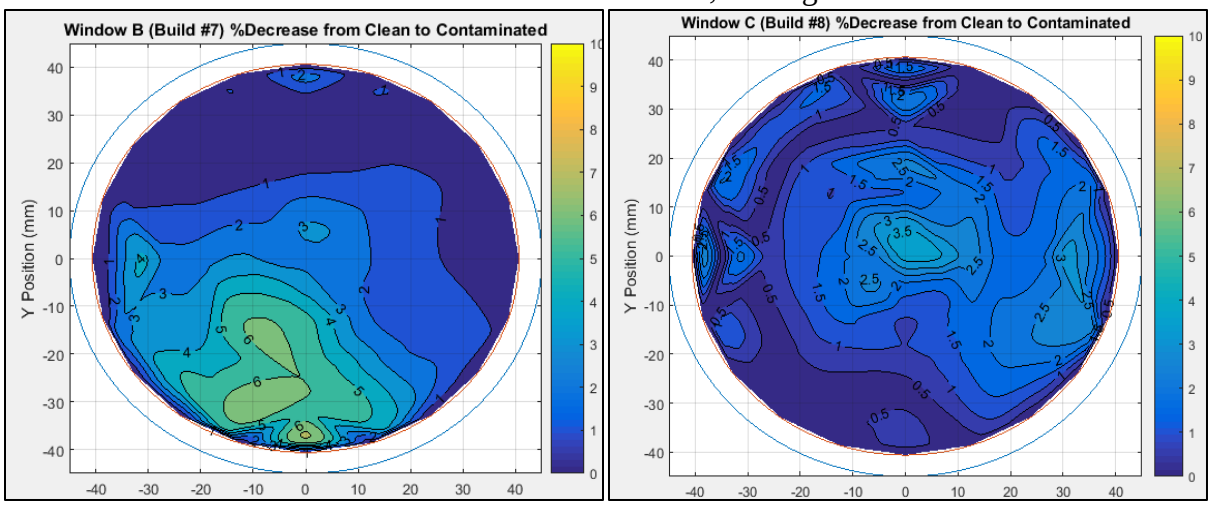

Figure 10: Contour plots of % change in attenuation from clean to contaminated windows

Again, the dissimilar pattern of contamination is apparent between the two windows. In addition, it should be noted that build #7 experienced laser power attenuated by ~6%, while the maximum attenuation in build #8 was ~3.5%. From Figure 10, it should be clear that a single-point measurement at the center of the window may not be indicative of contamination across the whole of the window. Table 2 compares the laser power attenuation due to contamination as measured by different methods.

Table 2: Comparison of measured attenuation by different measurement techniques

Laser Power Attenuation		
	Build #7	Build #8
Commercial Power meter*	1.71% ± 3%	0.75% ± 3%
Laser/photodiode**	2.53%± 0.51%	1.46 %± 0.51%
Laser/photodiode***	2.89% ± 0.51%	3.85%± 0.51%

*Requires 10+ samples taken to achieve better than manufacturer stated 3% uncertainty [10]
** Averaged over entire window
*** Sample taken only at center

When taking into account the associated uncertainties presented in Table 2, the percent attenuation measured for builds #7 and #8 is in support of some correlation between build height (number of layers) and contamination. In other words, because builds #7 and #8 were the same [height], their % attenuation should be statistically similar.

During an unrelated experiment using the Laser Additive Manufacturing Pilot System (LAMPS) at the University of Texas at Austin, infrared images (IR) were obtained showing

plumes of cool powder filling the build chamber during the powder drop before each layer, shown in Figure 11. These images suggest that the deposition/spreading of powder may be a cause of contamination, and would also support the claim of contamination on a per-layer basis.

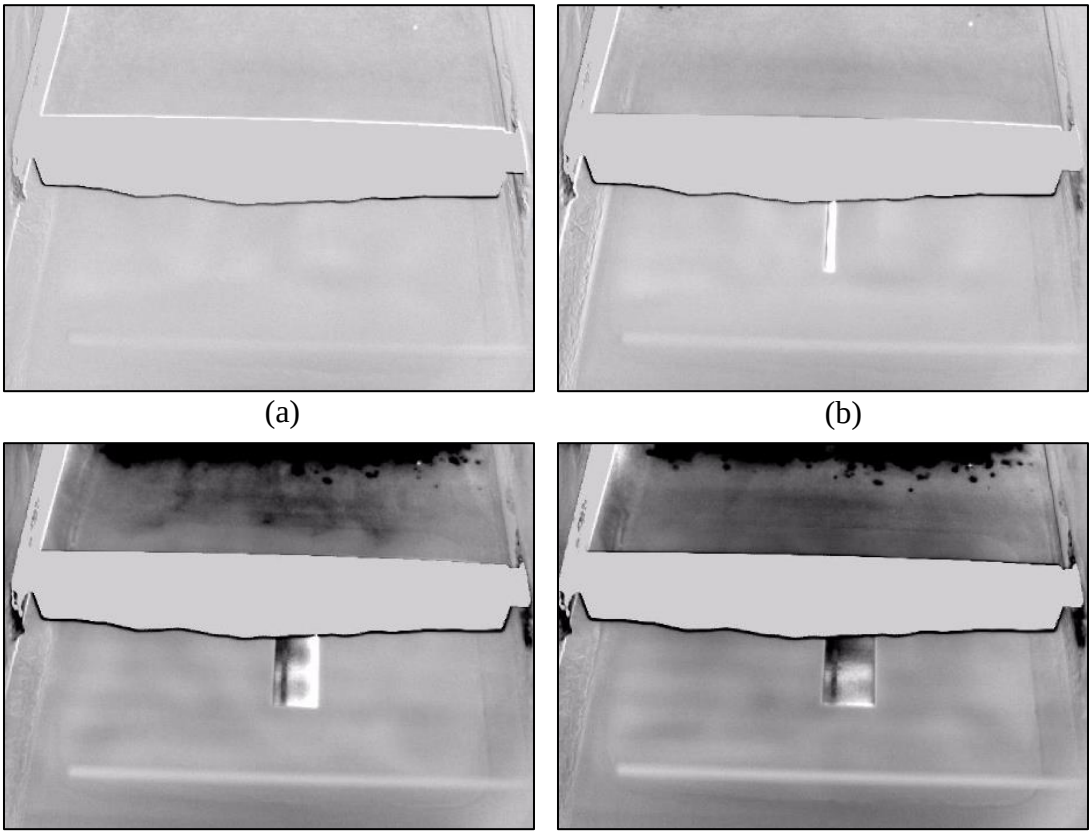

Figure 11: Thermal images of a pre-sintered powder bed (a), powder bed during sintering (b), powder drop from storage hopper (c), continued turbulence after powder drop (d)

Conclusion

Evidence has been presented that suggests laser window contamination in laser sintering is non-uniform across the window and non-repeatable from build-to-build or machine-to-machine. This result is suggestive of intra-layer variations in laser power attenuation (3.5%±0.25%), and therefore, correction via linear scaling of laser power on a layer-wise basis or a "standard power map" would likely be unsuccessful. In turn, simply measuring each window at one point before and after each build may not be sufficient for determining the level of contamination and a more robust measurement technique has been suggested.

Additionally, a correlation between laser window contamination and the number of layers in each build has been proposed, as measured by both a commercial power meter and low-cost variant. This claim was further supported with IR images of the powder deposition in a pilot SLS system at the University of Texas at Austin. The researchers have suggested that contamination likely occurs even during the pre-heat stage of a build, at which time a few layers of powder are deposited and the chamber temperature is elevated.

Future Work

Unfortunately, machine problems halted the progress towards predicting and correcting for window contamination via closed-loop control (CLC). However, work is underway to better understand the nature of contamination in hopes of developing a means to reduce or correct for it. In the near future, window contamination measurements will be taken before and after machine pre-heat to quantify the contamination occurring before LS. This process will be repeated for pre-heat + spreading of powder to determine the effects of powder spreading on laser window contamination. Finally, more production runs, similar to builds #7 and #8 above, will be executed and windows measured before and after to improve the statistics of 2D contamination variation.

References

[1] S. Taylor, J. Beaman and S. Fish, "Thermal History Correlation with Mechanical Properties for," in *SFF*, Austin, TX, 2017.

[2] W. Wroe, ""Improvements and Effects of Thermal History on Mechanical Properties for Polymer," University of Texas at Austin, Austin, TX, 2015.

[3] T. Phillips, A. McElroy, S. Fish and J. Beaman, "In-Situ Laser Control Method for Polymer," in *SFF*, Austin, TX, 2016.

[4] J. J. Beaman, "3D Printing Additive Manufacturing and Solid Freeform Fabrication: The Technologies of the Past Present and Future".

[5] B. Fulcher and D. Leigh, "Effects of Laser Window Degradation on Laser Power and Distribution in Laser Sintering," in *SFF*, Austin, TX, 2013.

[6] MatWeb, "ALM D80-ST Nylon 11 SLS Prototyping Polymer," MatWeb, [Online]. Available: http://www.matweb.com/search/datasheet.aspx?matguid=0343c74cf2c1462a988bafdc425a30d7&ckck=1. [Accessed 17 July 2018].

[7] MatWeb, "ALM FR 106 Nylon 11 SLS Prototyping Polymer," MatWeb, [Online]. Available: http://www.matweb.com/search/datasheet.aspx?matguid=20d35e23931d4d7eb964a31f0ad707e6. [Accessed 17 July 2018].

[8] D. Bourell, T. Watt, D. Leigh and B. Fulcher, "Performance Limitations in Polymer Laser Sintering," in *Photonic Technologies* , Furth, Germany, 2014.

[9] T. Diller, Y. Mengqi, D. Bourell and J. Beaman, "Thermal Model and Measurements of Polymer Laser Sintering," *Rapid Prototyping,* vol. 21, no. 1, pp. 2-13, 2012.

[10] R. J. Moffat, "Describing Uncertanties in Exp.l Results," *Exp.l Thermal and Fluid Sci.,* vol. 1, no. 1, 1988.